

**THE SUPERCRITICAL POMERON IN QCD\***Alan. R. White<sup>†</sup>

High Energy Physics Division  
Argonne National Laboratory  
9700 South Cass, Il 60439, USA.

**Abstract**

Deep-inelastic diffractive scaling violations have provided fundamental insight into the QCD pomeron, suggesting a single gluon inner structure rather than that of a perturbative two-gluon bound state. This talk outlines a derivation of a high-energy, transverse momentum cut-off, confining solution of QCD. The pomeron, in first approximation, is a single reggeized gluon plus a “wee parton” component that compensates for the color and particle properties of the gluon. This solution corresponds to a supercritical phase of Reggeon Field Theory.

Invited Talk Presented at the LAFEX International Workshop on Diffractive Physics,  
Rio de Janeiro, Brazil, February 16-20, 1998.

---

\*Work supported by the U.S. Department of Energy, Division of High Energy Physics,  
Contracts W-31-109-ENG-38 and DEFG05-86-ER-40272

<sup>†</sup>arw@hep.anl.gov

## 1 Introduction

A complete understanding of the pomeron in QCD requires the solution of the theory at high-energy. Although high-energy, perhaps, suggests a perturbative starting point, essential physics is clearly absent in the QCD perturbation expansion. In particular, it is well-established that confinement and chiral symmetry breaking are “low energy” properties that are essential in the physical solution of QCD but are not present in perturbation theory. We will also focus on two “high energy” experimental properties of the pomeron which are not present in perturbation theory. In small momentum transfer processes the pomeron is (approximately) a Regge pole, while in large  $Q^2$  deep-inelastic scattering it looks remarkably like a single gluon<sup>1</sup>. In this talk I will outline a high-energy solution of QCD in which these high energy properties of the pomeron are closely related to the low-energy “non-perturbative” properties of confinement and chiral symmetry breaking.

It is eighteen years since I first proposed<sup>2</sup> identifying a “supercritical phase” of Reggeon Field Theory (RFT) with a semi-perturbative picture of the QCD pomeron. The suggestion was that, in the supercritical phase, the “pomeron is a single (reggeized) gluon in a soft gluon background”. After many tries, I have finally found a detailed derivation<sup>3</sup> of this connection between RFT and the QCD pomeron. In this talk I will outline the derivation and show how the desired “non-perturbative” properties emerge.

In the course of this work I have gradually realized that many fundamental properties of the physical solution of QCD are deeply inter-related with the nature of the pomeron. As I will briefly elaborate at the end of this talk, I now believe that my pomeron solution also solves, in principle, the problem of finding a light-cone wee parton distribution for physical states which reproduces all the properties normally associated with a non-perturbative vacuum. Such a distribution is believed by many<sup>4</sup> to be behind the success of the constituent quark model in describing low-energy QCD. It also potentially provides a deeper origin of the parton model in QCD than that provided by the factorization properties of leading twist perturbation theory.

Multi-regge theory provides the framework for my analysis. By using reggeon unitarity equations<sup>5,6</sup> well-known Regge limit QCD calculations<sup>7,8,9</sup> can be extended to obtain multiparticle amplitudes involving multiple exchanges of reggeized gluons and quarks in a variety of Regge channels. In particular we can study amplitudes in which reggeon bound states and their scattering amplitudes appear. (Presently this is impossible in any other formalism.). In Fig. 1 we show qualitatively how we expect pion Regge pole amplitudes, for scattering via pomeron exchange, to emerge from the multiparticle reggeon diagrams describing the scattering of multi-quark states. We will find that new “reggeon helicity-flip” vertices that I have calculated play a vital dynamical role in such amplitudes.

In fact the hadron amplitudes we obtain are initially selected by a (“volume”) infra-red divergence that appears when SU(3) gauge symmetry is partially broken to SU(2) and the limit of zero quark mass is also taken. The divergence is produced by quark loop helicity-flip

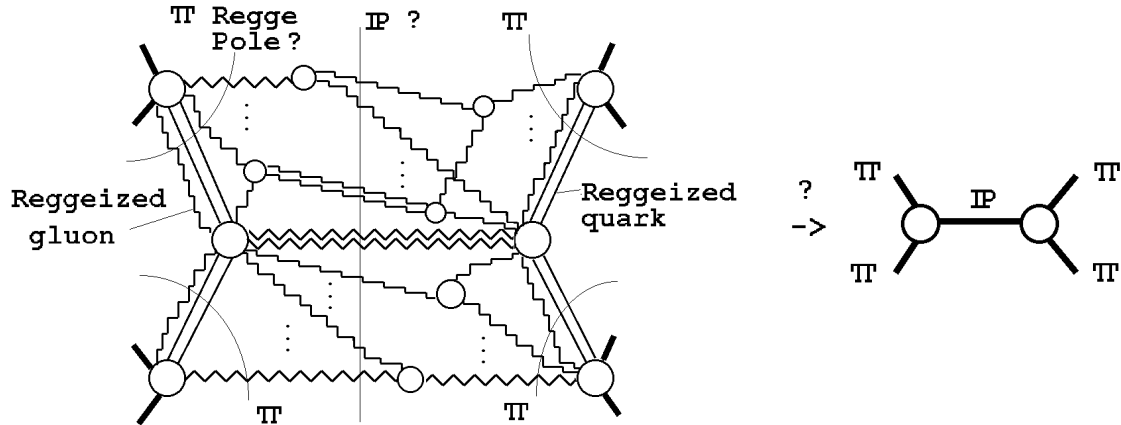


Fig. 1 The Anticipated Formation of Pion Scattering Amplitudes

vertices involving chirality violation (c.f. instanton interactions). The chirality violation survives the massless quark limit because of an infra-red effect of the triangle anomaly<sup>10</sup>. We show that the divergence produces what we will call a “wee parton condensate” which is directly responsible (when the gauge symmetry is partially broken) for confinement and chiral symmetry breaking. The pomeron is (in first approximation) a reggeized gluon in the wee parton condensate and so is obviously a Regge pole. Although we will not give any description of supercritical RFT<sup>6</sup> in this talk we do find that all the essential features are present. We briefly discuss the restoration of SU(3) gauge symmetry. It is closely related with the critical behaviour of the pomeron<sup>11</sup> and the consequent disappearance of the supercritical condensate. We note that the large  $Q^2$  of deep-inelastic scattering provides a finite volume constraint that can keep the theory (locally) in the supercritical phase as the full gauge symmetry is restored. A single gluon (in the background wee parton condensate) should then be a good approximation for the pomeron.

## 2 Multi-Regge Theory

This is an abstract formalism based on the existence of asymptotic analyticity domains for multiparticle amplitudes derived<sup>6,12</sup> via “Axiomatic Field Theory” and “Axiomatic S-Matrix Theory”. All the assumptions made are expected to be valid in a completely massive spontaneously-broken gauge theory. Since we begin with massive reggeizing gluons, this is effectively the starting point for our analysis of QCD. We can very briefly list the key ingredients as follows.

### *i) Angular Variables*

For an N-point amplitude we can introduce variables corresponding to any Toller diagram, i.e. any tree diagram, drawn as in Fig. 2, that involves only three-point vertices. The result

is that we can write

$$M_N(P_1, \dots, P_N) \equiv M_N(t_1, \dots, t_{N-3}, g_1, \dots, g_{N-3})$$

where  $t_j = Q_j^2$  and  $g_j$  is in the little group of  $Q_j$ , i.e. for  $t_j > 0$ ,  $g_j \in \text{SO}(3)$ , and for  $t_j < 0$ ,  $g_j \in \text{SO}(2,1)$ . A set of  $3N - 10$  independent variables is obtained,  $N-3$   $t_i$  variables,  $N-3$   $z_j$  ( $\equiv \cos \theta_j$ ) variables and  $N-4$   $u_{jk}$  ( $\equiv e^{i(\mu_j - \nu_k)}$ ) variables.

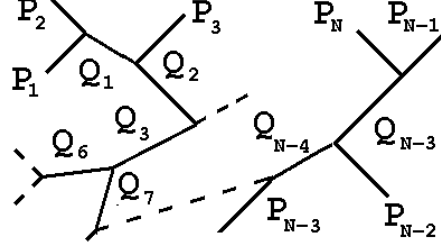


Fig. 2 A Tree Diagram with Three Point Vertices.

#### ii) Multi-Regge Limits

These limits are defined by  $z_j \rightarrow \infty$ ,  $\forall j$ . We will also be interested in *Helicity-Pole Limits* in which some  $u_{jk} \rightarrow \infty$  and some  $z_j \rightarrow \infty$ . In a helicity-pole limit a smaller number of invariants is taken large.

#### iii) Partial-wave Expansions

Using  $f(g) = \sum_{J=0}^{\infty} \sum_{|n|, |n'| < J} D_{nn'}^J(g) a_{Jnn'}$ , for a function  $f(g)$  defined on  $\text{SO}(3)$ , leads to

$$M_N(t, g) = \sum_{J, n, n'} \prod_i D_{n_i n'_i}^{J_i}(g_i) a_{J, n, n'}(t)$$

#### iv) Asymptotic Dispersion Relations

We can write  $M_N = \sum_C M_N^C + M^0$  where

$$M_N^C = \frac{1}{(2\pi i)^{N-3}} \int \frac{ds'_1 \dots ds'_{N-3} \Delta^C(\dots t_i, \dots u_{jk}, \dots s'_i)}{(s'_1 - s_1)(s'_2 - s_2) \dots (s'_{N-3} - s_{N-3})}$$

and  $\sum_C$  is over all sets of  $(N-3)$  Regge limit asymptotic cuts.  $M^0$  is non-leading in the multi-regge limit. The resulting separation into (hexagraph) spectral components is crucial for the development of multiparticle complex angular momentum theory.

#### v) Sommerfeld-Watson Representations of Spectral Components

A multiple transformation of the partial-wave expansion gives e.g.

$$M_4^C = \frac{1}{8} \sum_{N_1, N_2} \int \frac{dn_2 dn_1 dJ_1 u_2^{n_2} u_1^{n_1} d_{0, n_1}^{J_1}(z_1) d_{n_1, n_2}^{n_1 + N_2}(z_2) d_{n_2, 0}^{n_2 + N_3}(z_3)}{\sin \pi n_2 \sin \pi(n_1 - n_2) \sin \pi(J_1 - n_1)} a_{N_2 N_3}^C(J_1, n_1, n_2, t) \\ + \sum_{\tilde{J}, \tilde{n}}^{\sim} d_{0, n_1}^{\tilde{J}_1}(z_1) u_1^{n_1} d_{n_1, n_2}^{\tilde{J}_2}(z_2) u_2^{n_2} d_{n_2, 0}^{\tilde{J}_3}(z_3) a_{\tilde{J}, \tilde{n}}(\tilde{t})$$

These representations give the form of the asymptotic behaviour in both multi-Regge and helicity-pole limits. In particular, in a “maximal” helicity-pole limit, in which the maximal number of  $u_{jk} \rightarrow \infty$ , only a single (analytically-continued) partial-wave amplitude appears.

vi) *t-channel Unitarity in the J-plane*

Multiparticle unitarity in every  $t$ -channel can be partial-wave projected, diagonalized, and continued to complex  $J$  as an equation for partial-wave amplitudes, i.e.

$$a_J^+ - a_J^- = i \int d\rho \sum_{\tilde{N}} \int \frac{dn_1 dn_2}{\sin \pi(J - n_1 - n_2)} \int \frac{dn_3 dn_4}{\sin \pi(n_1 - n_3 - n_4)} \cdots a_{J\tilde{N}\tilde{n}}^+ a_{J\tilde{N}\tilde{n}}^-$$

Regge poles at  $n_i = \alpha_i$ , together with the phase-space  $\int d\rho$  and the “nonsense poles” at  $J = n_1 + n_2 - 1, n_1 = n_3 + n_4 - 1, \dots$  generate multi-reggeon thresholds, i.e. Regge cuts.

vii) *Reggeon Unitarity*

In ANY  $J$ -plane of any partial-wave amplitude, the “threshold” discontinuity due to  $M$  Regge poles with trajectories  $\alpha = (\alpha_1, \alpha_2, \dots, \alpha_M)$  is given by the reggeon unitarity equation

$$\text{disc}_{J=\alpha_M(t)} a_{N\tilde{n}}(J) = \xi_M \int d\hat{\rho} a_{\alpha}(J^+) a_{\alpha}(J^-) \frac{\delta \left( J - 1 - \sum_{k=1}^M (\alpha_k - 1) \right)}{\sin \frac{\pi}{2}(\alpha_1 - \tau'_1) \dots \sin \frac{\pi}{2}(\alpha_M - \tau'_M)}$$

Writing  $t_i = k_i^2$  (with  $\int dt_1 dt_2 \lambda^{-1/2}(t, t_1, t_2) = 2 \int d^2 k_1 d^2 k_2 \delta^2(k - k_1 - k_2)$ ),  $\int d\hat{\rho}$  can be written in terms of two dimensional “ $k_\perp$ ” integrations, anticipating the reggeon diagram results of direct  $s$ -channel high-energy calculations<sup>7,8,9</sup>. The generality of reggeon unitarity makes it particularly powerful when applied to the partial-wave amplitudes appearing in maximal helicity-pole limits.

### 3 Reggeon Diagrams in QCD

Leading-log Regge limit calculations of elastic and multi-regge production amplitudes in (spontaneously-broken) gauge theories show<sup>7,8,9</sup> that both gluons and quarks “reggeize”, i.e. they lie on Regge trajectories. Non-leading log calculations are described by “reggeon diagrams” involving reggeized gluons and quarks. In fact, reggeon unitarity requires that higher-order calculations produce a complete set of reggeon diagrams.

Gluon reggeon diagrams involve a reggeon propagator for each reggeon state and also gluon particle poles e.g.

$$\text{two-reggeon state} \leftrightarrow \int \frac{d^2 k_1}{(k_1^2 + M^2)} \frac{d^2 k_2}{(k_2^2 + M^2)} \frac{\delta^2(k'_1 + k'_2 - k_1 - k_2)}{J - 1 + \Delta(k_1^2, M^2) + \Delta(k_2^2, M^2)}$$

The BFKL equation<sup>7</sup> corresponds to 2-reggeon unitarity, i.e. iteration of the color-zero 2-reggeon state with the 2-2 reggeon interaction

$$\Gamma_{22}(\underline{k}_1, \underline{k}_2, \underline{k}'_1, \underline{k}'_2, M^2) = \frac{(\underline{k}_1^2 + M^2)(\underline{k}_2'^2 + M^2) + (\underline{k}_2^2 + M^2)(\underline{k}_1'^2 + M^2)}{(\underline{k}_1 - \underline{k}'_1)^2 + M^2} + \dots$$

We are interested in the infra-red limit in which the gluon mass  $M \rightarrow 0$ . We will, effectively, assume that two well-known leading-order properties of this limit generalize to all orders. The first property is that infra-red divergences, due to the gluon particle poles in the reggeon states, interactions, and trajectory function, exponentiate to zero all diagrams that do not carry zero color in the  $t$ -channel. The second property (which actually requires appropriate behavior of the gauge coupling in higher orders) is that the infra-red finiteness of color-zero reggeon interactions implies canonical scaling ( $\sim Q^{-2}$ ) for color zero reggeon amplitudes in the limit that all internal transverse momenta are scaled to zero.

#### 4 Reggeon Diagrams for Helicity-Pole Limit Amplitudes

For our purposes, “maximal” helicity-pole limits of multiparticle amplitudes are the most interesting to study. Because the Sommerfeld-Watson representation involves only a single partial-wave amplitude, reggeon unitarity straightforwardly implies that reggeon diagrams again appear. (Although <sup>3</sup> “physical”  $k_\perp$  planes in general contain lightlike momenta !)

As an example, we introduce variables for the 8-pt amplitude corresponding to the tree diagram of Fig. 3. We consider the “helicity-flip” limit

$$z, u_1, u_2^{-1}, u_3, u_4^{-1} \rightarrow \infty$$

(In this example,  $u_1, u_2^{-1} \rightarrow \infty$  is a helicity-flip limit, while  $u_1, u_2 \rightarrow \infty$  is a non-flip limit.) The behavior of invariants is

$$\begin{aligned} P_1.P_2 &\sim u_1 u_2^{-1}, & P_1.P_3 &\sim u_1 z u_3, \\ P_2.P_4 &\sim u_2^{-1} u_4^{-1}, & P_1.Q_3 &\sim u_1 z, \\ Q_1.Q_3 &\sim z, & P_4.Q_1 &\sim z u_4^{-1} \dots \\ P_1.Q, P_2.Q, P_3.Q, P_4.Q & \text{finite} \end{aligned}$$

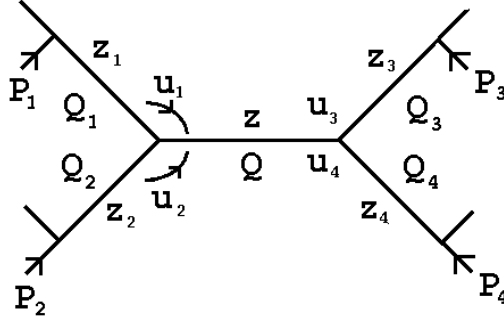


Fig. 3 Variables for the 8-pt Amplitude

Reggeon unitarity determines that the helicity-flip limit is described by reggeon diagrams of the form shown in Fig. 4.  $\textcircled{A}$  contains all elastic scattering reggeon diagrams. The  $T^F$  are new “reggeon helicity-flip” vertices that play a crucial role in our QCD analysis. (These vertices do not appear in elastic scattering reggeon diagrams).

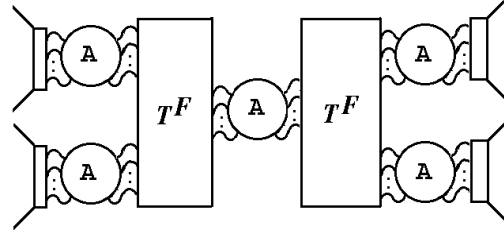


Fig. 4 Reggeon Diagrams for the 8-pt Amplitude

## 5 Reggeon Helicity-Flip Vertices

The  $T^F$  vertices are most simply isolated kinematically by considering a “non-planar” triple-regge limit which, for simplicity, we will define by introducing three distinct light-cone momenta. (This limit actually gives a sum of three  $T^F$  vertices of the kind discussed above<sup>3</sup>, but in this talk we will not elaborate this subtlety.) We use the tree diagram of Fig. 5(a) to define momenta and study the special kinematics

$$P_1 \rightarrow (p_1, p_1, 0, 0), \quad p_1 \rightarrow \infty$$

$$P_2 \rightarrow (p_2, 0, p_2, 0), \quad p_2 \rightarrow \infty$$

$$P_3 \rightarrow (p_3, 0, 0, p_3), \quad p_3 \rightarrow \infty$$

$$Q_1 \rightarrow (0, 0, q_2, -q_3)$$

$$Q_2 \rightarrow (0, -q_1, 0, q_3)$$

$$Q_3 \rightarrow (0, q_1, -q_2, 0)$$

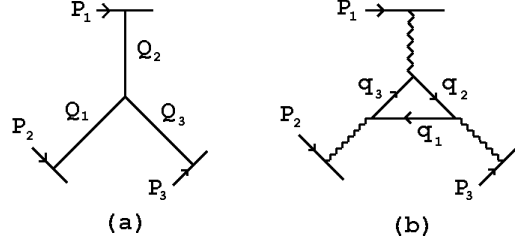


Fig. 5 (a) A Tree Diagram and (b) a quark loop coupling for three quark scattering.

We consider three quarks scattering via gluon exchange with a quark loop coupling as in Fig. 5(b). The non-planar triple-regge limit

$$\rightarrow g^6 \frac{p_1 p_2 p_3}{t_1 t_2 t_3} \Gamma_{1+2+3+}(q_1, q_2, q_3) \leftrightarrow g^3 \frac{p_1 p_2 p_3}{t_1 t_2 t_3} T^F(Q_1, Q_2, Q_3)$$

where  $\gamma_{i+} = \gamma_0 + \gamma_i$  and  $\Gamma_{\mu_1 \mu_2 \mu_3}$  is given by the quark triangle diagram i.e.

$$\Gamma_{\mu_1 \mu_2 \mu_3} = i \int \frac{d^4 k \text{Tr}\{\gamma_{\mu_1}(\not{q}_3 + \not{k} + m)\gamma_{\mu_2}(\not{q}_1 + \not{k} + m)\gamma_{\mu_3}(\not{q}_2 + \not{k} + m)\}}{[(q_1 + k)^2 - m^2][(q_2 + k)^2 - m^2][(q_3 + k)^2 - m^2]}$$

where  $m$  is the quark mass. We denote the  $O(m^2)$  chirality-violating part of  $T^F$  ( $\equiv g^3 \Gamma_{1+2+3+}$ ) by  $T^{F,m^2}$  and note that the limits  $q_1, q_2, q_3 \sim Q \rightarrow 0$  and  $m \rightarrow 0$  do not commute, i.e.

$$T^{F,m^2} \underset{Q \rightarrow 0}{\sim} Q i m^2 \int \frac{d^4 k}{[k^2 - m^2]^3} = R Q$$

where  $R$  is independent of  $m$ . This non-commutativity is an “infra-red anomaly” due to the triangle Landau singularity<sup>10</sup>.

$T^F$  is also ultra-violet divergent. It is one of a general set of quark loop reggeon interactions that have ultra-violet divergences and so require regularization. We do this by introducing Pauli-Villars fermions that maintain the reggeon Ward identities that ensure gauge invariance<sup>3</sup>. (Note that we take the regulator mass  $m_\Lambda \rightarrow \infty$  after  $m \rightarrow 0$ . This implies that the initial theory with  $m \neq 0$  is non-unitary for  $k_\perp \gtrsim m_\Lambda$ .) For the regulated

vertex,  $T^{\mathcal{F},m^2}$ , we obtain (for  $m \neq 0$ )

$$T^{\mathcal{F},m^2}(Q) \sim T^{F,m^2} - T^{F,m_\Lambda^2} \sim Q^2 \quad Q \rightarrow 0$$

However, since  $T^{F,0} = 0$ , we also have

$$T^{\mathcal{F},0}(Q) \sim -R Q \quad Q \rightarrow 0$$

showing that imposing reggeon Ward identities for  $m \neq 0$  leads to a slower vanishing as  $Q \rightarrow 0$  when  $m = 0$ .

After color factors are included and all diagrams summed, we find that  $T^{\mathcal{F},0}(Q)$  survives only in very special reggeon vertices, i.e. vertices coupling reggeon states with “anomalous color parity”. We define color parity ( $C_c$ ) via the transformation

$$A_{ab}^i \rightarrow -A_{ba}^i$$

for gluon color matrices. We say that a reggeon state has anomalous color parity if the signature ( $\tau$ ), determined by whether the number of reggeons is even or odd, is not equal to the color parity. (Note that the reggeized gluon and the BFKL two reggeon state both have normal color parity.)

We will be particularly interested in the “anomalous odderon” three-reggeon state with color factor  $f_{ijk}A^iA^jA^k$  that has  $\tau = -1$  but  $C_c = +1$  (c.f. the winding-number current  $K_\mu = \epsilon_{\mu\nu\gamma\delta}f_{ijk}A_\nu^iA_\gamma^jA_\delta^k$ ).  $T^{\mathcal{F},0}(Q)$

appears in the triple coupling of three anomalous odderon states as in Fig. 6. The quantum numbers of the anomalous odderon state imply that, in this case, the survival of  $O(m^2)$  processes as  $m \rightarrow 0$  could be reproduced by the chirality violation of instanton interactions. In

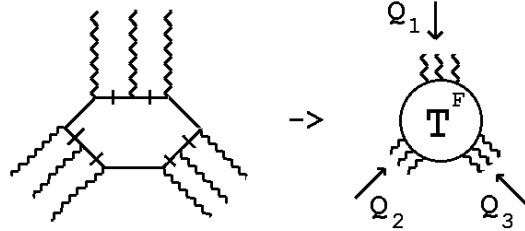


Fig. 6 An Anomalous Odderon Triple Coupling.

our case the presence of such non-perturbative interactions in the massless theory is due to our regularization procedure for reggeon interaction vertices.

## 6 A Quark Mass Infra-Red Divergence

A vital consequence of the “anomalous” behavior of  $T^{\mathcal{F},0}$  as  $Q \rightarrow 0$  is that an additional infra-red divergence is produced (as  $m \rightarrow 0$ ) in massless gluon reggeon diagrams.



The divergence occurs in diagrams involving the  $T^F$  where  $Q_1 \sim Q_2 \sim Q_3 \sim 0$  is part of the integration region. However, the  $T^F$  only appear in vertices coupling distinct reggeon channels. A potentially divergent diagram containing  $T^F$  vertices is shown in Fig. 7. In this diagram an anomalous odderon reggeon state is denoted by  $\text{---} = \text{---}$  while  $\text{---}$  denotes any normal reggeon state. Fig. 7 is of the general form illustrated in Fig. 4, except that we are allowing the vertices  $V_i$  to involve more complicated external states than a single scattering quark. The canonical scaling of the anomalous odderon states gives the infra-red behaviour

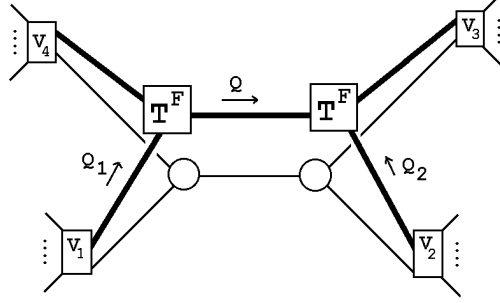



Fig. 7 A Divergent Reggeon Diagram

$$\int \dots \frac{d^2 Q_1}{Q_1^2} \frac{d^2 Q_2}{Q_2^2} \frac{d^2 Q}{Q^2 (Q - Q_1)^2 (Q - Q_2)^2} \\ \times V_1(Q_1) V_2(Q_2) V_3(Q - Q_2) V_4(Q - Q_1) T^F(Q_1, Q) T^F(Q, Q_2) \\ \times [\text{regular vertices and reggeon propagators}]$$

Depending on the behaviour of the  $V_i$  it appears that a divergence potentially occurs when  $Q \sim Q_1 \sim Q_2 \rightarrow 0$ . However, in general gauge invariance produces<sup>3</sup> a cancelation of this divergence by a similar divergence of diagrams related to that of Fig. 7 by reggeon Ward identities for the reggeons within the anomalous odderon states.

We can preserve the divergence of the diagram of Fig. 7 and eliminate the possibility of a cancelation if we partially break the SU(3) gauge symmetry to SU(2). In effect, introducing the symmetry breaking mass scale provides a scale for the logarithmic quark mass divergence. (Note also that the topology of an instanton is defined with respect to an SU(2) subgroup. As a result we anticipate that this partial breaking enhances the significance of topological effects associated with the anomaly.) We can show that other diagrams can not cancel the quark mass divergence discussed above if  $\text{---}$  is any SU(2) singlet combination of massless gluons with  $C_c = -\tau = +1$  (i.e. a generalized SU(2) anomalous odderon) and  $\text{---}$  is a normal reggeon state containing one or more SU(2) singlet massive reggeized gluons (or quarks). We can then regard Fig. 7 as containing only reggeon states of the form  $\text{---}$  coupling via a combination of regular and  $T^{\mathcal{F},0}$  vertices.


We must also discuss specifically the behavior of the  $V_i$ . A-priori reggeon Ward identities imply  $V_i \rightarrow 0$  when  $Q_i \rightarrow 0$ . This, in itself, would be sufficient to eliminate any divergence in Fig. 7! However, if we impose the “initial condition” that  $V_1, V_2 \not\rightarrow 0$ , the divergence is present and in fact occurs similarly in a general class of diagrams, as we now discuss. We

consider a diagram having the general structure illustrated in Fig. 8, in which there are  $n + 3$  multi-reggeon states of the form . Imposing  $V_1, V_2 \not\rightarrow 0$  and assuming that reggeon Ward identities are satisfied by the remaining vertices, i.e.

$$V_i(Q_i) \sim V(Q_i) = Q_i$$

$i \neq 1, 2$ , gives that Fig. 8 has the infra-red behavior

$$\int \frac{d^2 Q}{Q^2} \left[ \int \frac{d^2 Q}{Q^4} \right]^n \times [V(Q) T^{\mathcal{F}}(Q)]^n$$

Thus giving (as  $m \rightarrow 0$ ) an overall logarithmic divergence. In general, this divergence occurs in just those multi-reggeon diagrams which contain only SU(2) color zero states of the form  coupled by regular and  $T^{\mathcal{F},0}$  vertices, as in the examples we have discussed.

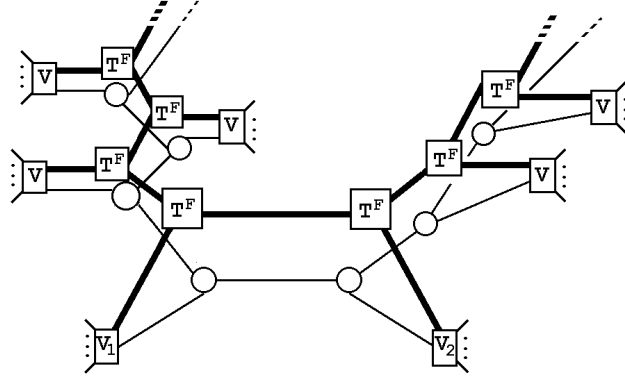


Fig. 8 A General Divergent Diagram

## 7 Confinement and a Parton Picture

We define physical amplitudes from divergent diagrams by extracting the coefficient of the logarithmic divergence. The resulting reggeon states and amplitudes produce “a confinement phenomenon” in the following sense. A particular set of color-zero reggeon states is selected that contains no massless multigluon states and has the necessary completeness property to consistently define an S-Matrix. By completeness we mean that if two or more of this set of states initially scatter via QCD interactions, the final states contain only arbitrary numbers of the same set of states. Since the divergence involves zero  $k_{\perp}$  for the anomalous odderon component of each reggeon state, an “anomalous odderon condensate” is generated. The general picture is illustrated in Fig. 9. In addition to the zero  $k_{\perp}$  (or wee-parton) component, physical reggeon states have a finite momentum “normal” parton component carrying the kinematic properties of interactions. We emphasize that the “scattering” of the  $k_{\perp} = 0$  condensate is directly due to the infra-red quark triangle anomaly.

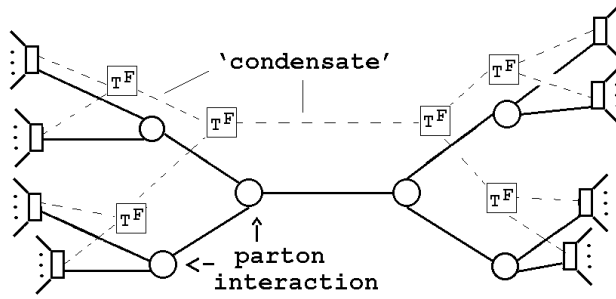


Fig. 9 The Parton Picture

The breaking of the gauge symmetry has produced physical states in which the “partons” are separated into a universal wee-parton component and a normal reggeon parton component which is distinct in each distinct physical state. However, the condensate has the important property that it switches the signature compared to that of the normal parton component. We note the following important reggeon states.

- There is a “pomeron” whose normal parton component is a reggeized gluon. This is a Regge pole with  $\tau = -C_c = +1$  and intercept  $\neq 0$ .
- A bound-state reggeon formed from two massive SU(2) doublet gluons gives an exchange-degenerate partner to the pomeron, i.e. a Regge pole with  $\tau = -C_c = -1$ . The SU(2) singlet massive gluon lies on this trajectory.
- “Hadrons” have a constituent quark normal parton component.

All the features of supercritical RFT are present, but we will not discuss the details. Although we have not specifically discussed quark reggeons, the hadron reggeons they form are vital. “Stability” of the quark parton component within the condensate produces chiral symmetry breaking, which determines that hadrons are not eigenstates of color parity. This is necessary if the exchange of a pomeron with  $C_c = -1$  is to describe elastic scattering.

## 8 Restoration of SU(3) Gauge Symmetry

We make only a few brief comments on this, obviously important, subject. Because of complementarity<sup>13</sup>, restoring SU(3) symmetry (which involves decoupling a color triplet Higgs scalar field) should be straightforward if we impose a transverse momentum cut-off  $k_\perp < \Lambda_\perp$ . Restoring the symmetry involves removing the mass scale that distinguishes normal (finite momentum) partons from wee (zero momentum) partons and produces the reggeon condensate. Mapping the (partially) broken theory completely onto supercritical RFT implies that the condensate and the odd-signature partner for the pomeron disappear simultaneously. The result is then the critical pomeron<sup>11</sup>. The wee-parton condensate will be replaced by a small  $k_\perp$ , wee parton, critical phenomenon that merges smoothly with the large  $k_\perp$  normal (or constituent) parton component of physical states, just as originally envisaged by Feynman<sup>14</sup>. (Note that, because of the odd SU(3) color charge parity of the pomeron, the two-gluon BFKL pomeron will not be involved.)

Mapping partially-broken QCD onto supercritical RFT has further consequences. In particular, it implies that the  $\Lambda_\perp$  scale mixes with the symmetry breaking scale and becomes a “relevant parameter” for the critical behavior. It then follows that, after the symmetry breaking scale is removed, there will (for a general number of quark flavors) be a  $\Lambda_{\perp c}$  such that  $\Lambda_\perp > \Lambda_{\perp c}$  implies the pomeron is in the subcritical phase, while  $\Lambda_\perp < \Lambda_{\perp c}$  implies it is in the supercritical phase. We conclude that the supercritical phase can be realized with the gauge symmetry restored if  $\Lambda_\perp$  is taken small enough. However,  $\alpha_{\mathbb{P}}(0)$  and the mass of the exchange degenerate, composite, “reggeized gluon” will be functions of  $\Lambda_\perp$ . In

deep-inelastic diffraction, large  $Q^2$  will act as a (local) lower  $k_\perp$  cut-off and produce a “finite volume” effect that can keep the theory supercritical as the SU(3) symmetry is restored.

To remove  $\Lambda_\perp$  requires  $\Lambda_{\perp c} = \infty$ . We will not discuss here why we believe this requires a specific quark flavor content. It is interesting that, for any quark content, we can take  $\Lambda_\perp \ll \Lambda_{\perp c}$ , and go deep into the supercritical phase. We obtain a picture in which constituent quark hadrons interact via a massive composite “gluon” (and an exchange degenerate pomeron). Confinement and chiral symmetry breaking are realized via a simple, universal, wee parton component of physical states. This is remarkably close to the realization of the constituent quark model via light-cone quantization that has been advocated by light-cone enthusiasts<sup>4</sup>.

## References

1. H1 Collaboration, pa02-61 ICHEP’96 (1996), For a final version of the analysis see *Z. Phys.* **C76**, 613 (1997).
2. A. R. White, CERN preprint TH.2976 (1980). A summary of this paper is presented in the Proceedings of the XVIth Rencontre de Moriond, Vol. 2 (1981).
3. A. R. White, hep-ph/9712466 (1997).
4. K. G. Wilson, T. S. Walhout, A. Harindranath, Wei-Min Zhang, S. D. Glazek and R. J. Perry, *Phys. Rev.* **D 49**, 6720 (1994); L. Susskind and M. Burkardt, hep-ph/9410313 (1994).
5. V. N. Gribov, I. Ya. Pomeranchuk and K. A. Ter-Martirosyan, *Phys. Rev.* **139B**, 184 (1965).
6. A. R. White, *Int. J. Mod. Phys.* **A11**, 1859 (1991); A. R. White in *Structural Analysis of Collision Amplitudes*, (North Holland, 1976).
7. E. A. Kuraev, L. N. Lipatov, V. S. Fadin, *Sov. Phys. JETP* **45**, 199 (1977) ; Ya. Ya. Balitsky and L. N. Lipatov, *Sov. J. Nucl. Phys.* **28**, 822 (1978). V. S. Fadin and L. N. Lipatov, *Nucl. Phys.* **B477**, 767 (1996) and further references therein.
8. J. B. Bronzan and R. L. Sugar, *Phys. Rev.* **D17**, 585 (1978). This paper organizes into reggeon diagrams the results from H. Cheng and C. Y. Lo, *Phys. Rev.* **D13**, 1131 (1976), **D15**, 2959 (1977).
9. V. S. Fadin and V. E. Sherman, *Sov. Phys. JETP* **45**, 861 (1978).
10. S. Coleman and B. Grossman, *Nucl. Phys.* **B203**, 205 (1982).
11. A. A. Migdal, A. M. Polyakov and K. A. Ter-Martirosyan, *Zh. Eksp. Teor. Fiz.* **67**, 84 (1974); H. D. I. Abarbanel and J. B. Bronzan, *Phys. Rev.* **D9**, 2397 (1974).
12. H. P. Stapp in *Structural Analysis of Collision Amplitudes*, (North Holland, 1976); H. P. Stapp and A. R. White, *Phys. Rev.* **D26**, 2145 (1982).
13. E. Fradkin and S. H. Shenker, *Phys. Rev.* **D19**, 3682 (1979); T. Banks and E. Rabinovici, *Nucl. Phys.* **B160**, 349 (1979).
14. R. P. Feynman in *Photon Hadron Interactions* (Benjamin, 1972)).